

Tensor Factorization and Continuous Wavelet Transform for Model-free Single-Frame Blind Image Deconvolution

Ivica Kopriva

Ruđer Bošković Institute
Bijenička cesta 54
10000 Zagreb, Croatia
ikopriva@irb.hr

Qian Du

Department of Electrical and Computer Engineering
Mississippi State University
MS 39762, USA
du@ece.msstate.edu

Abstract— **Model-free single-frame blind image deconvolution (BID) method is proposed by converting BID into blind source separation (BSS), whereas sources represent the original image and its spatial derivatives. Continuous wavelet transform (CWT) is used to generate multi-channel image necessary for BSS. As opposed to an approach based on the Gabor filter bank, this brings additional options in adaptability to the problem at hand: through the choice of wavelet function and variation of the scale of the CWT. BSS is performed through orthogonality constrained factorization of the 3D multichannel image tensor by means of the higher-order-orthogonal-iteration algorithm. The proposed method virtually requires no information about blurring kernel: neither model nor size of the support. The method is demonstrated on experimental gray scale images degraded by de-focusing and atmospheric turbulence. A comparable or better performance is demonstrated relative to blind Richardson-Lucy method that, however, requires a priori information about parametric model of the blur.**

I. INTRODUCTION

Degradation of the spatial resolution of an image is caused by various sources (either individually or combined): atmospheric turbulence, defocusing, relative motion between image and object planes, aberrations, etc. Restoration of the original image from its blurred version is referred to as image restoration or image deconvolution [1, 2]. In non-blind deconvolution the blurring kernel is given [1], while in blind deconvolution it is unknown [2]. In majority of the cases it is, however, assumed that parametric model of the blurring kernel is known which leads to model-based blind image deconvolution (BID) [3-5]. This however presumes that source of the image degradation is known and that is not always the case in practice. Also, it is not always possible to have at disposal multiple frames as required by multi-frame BID [3,4]. Due to these reasons it has been exploited previously whether single-frame model-free BID problem is possible to solve? To this end, several algorithms for single-frame model-free BID have been demonstrated [6-10]. All these approaches have in common the following features: (1) BID is converted into BSS problem through the implicit use of the Taylor expansion of the shifted original image around origin in the image forming convolution equation [11]; (2) Gabor filter bank is used to generate multichannel version of

the single-frame image. Hence, it is implicitly assumed that original image has certain degree of smoothness that limits performance of model-free BID in scenarios where degradation is strong and/or original image is composed of sharp edges [10].

Herein, we propose continuous wavelet transform (CWT) [12] as a substitute for Gabor filter bank with the following improvements: (1) since scale of the CWT is continuous, number of multichannel images can be varied by varying resolution and support of the scale; (2) selection of wavelet function gives additional degree of adaptability to the problem at hand. Since in considered problem sources represent original image and its spatial derivatives they are neither sparse nor statistically independent. Therefore, sparseness [6] and statistical independence [7] based approaches yield suboptimal result in multi-frame BID problem. Therefore, as in [9,10] we use tensor factorization (TF) with orthogonality constraints imposed on the factors and core tensor of the Tucker3 model of the multichannel image tensor. In comparison with the independent and sparse component analysis, TF approach yields constraints-relaxed solution of the model-free BID problem. The rest of the paper is organized as follows. Model-free BID problem with the TF based solution is formulated in section 2, and the CWT-based multichannel image generation is presented in section 3. The proposed method is demonstrated on experimental gray scale images degraded by defocusing and atmospheric turbulence in section 4, while conclusions are drawn in section 5.

II. MODEL-FREE BLIND IMAGE DECONVOLUTION

It is assumed that blurred gray scale image $\mathbf{G} \in R_{0+}^{I_1 \times I_2}$, with I_1 and I_2 representing number of pixels, is degraded by space-invariant blur, also known as point spread function (PSF), and described by linear image forming convolution equation:

$$\mathbf{G}(i_1, i_2) = \sum_{s=-M}^M \sum_{t=-M}^M \mathbf{H}(s, t) \mathbf{F}(i_1 - s, i_2 - t) \quad (1)$$

where M denotes half of the PSF support size. In equation (1) presence of the additive noise is ignored in order to focus on an essential issue: model-free BID. It is also assumed that the unknown original image \mathbf{F} is n^{th} order smooth implying that it

is n -times differentiable at the origin (i_1, i_2) , whereupon n represents the order of spatial derivatives (terms) in the Taylor expansion of $\mathbf{F}(i_1 - s, i_2 - t)$ around the origin (i_1, i_2) . An implicit Taylor expansion of the original image $\mathbf{F}(i_1 - s, i_2 - t)$ around (i_1, i_2) , is used to convert BID into BSS, [11] yielding:

$$\mathbf{F}(i_1 - s, i_2 - t) = \mathbf{F}(i_1, i_2) - s\mathbf{F}_{i_1}(i_1, i_2) - t\mathbf{F}_{i_2}(i_1, i_2) + \frac{1}{2}s^2\mathbf{F}_{i_1 i_1}(i_1, i_2) + \frac{1}{2}t^2\mathbf{F}_{i_2 i_2}(i_1, i_2) + \frac{1}{2}st\mathbf{F}_{i_1 i_2}(i_1, i_2) - \dots \quad (2)$$

where \mathbf{F}_{i_1} , \mathbf{F}_{i_2} , $\mathbf{F}_{i_1 i_1}$, $\mathbf{F}_{i_2 i_2}$ and $\mathbf{F}_{i_1 i_2}$ are first- and second-order spatial derivatives in i_1 and i_2 directions respectively. By using (2) equation (1) can be re-written as:

$$\mathbf{G}(i_1, i_2) = a_1\mathbf{F}(i_1, i_2) - a_2\mathbf{F}_{i_1}(i_1, i_2) - a_3\mathbf{F}_{i_2}(i_1, i_2) + a_4\mathbf{F}_{i_1 i_1}(i_1, i_2) + a_5\mathbf{F}_{i_2 i_2}(i_1, i_2) + a_6\mathbf{F}_{i_1 i_2}(i_1, i_2) - \dots \quad (3)$$

The unknown weighting coefficients in (3) are straightforward to derive and are given in [6,7]. It is of great importance to note that blurred image (3) represents a linear combination of the original image and its spatial derivatives. The unknown weighting coefficients a_1 to a_6 absorbed into themselves the coefficients of the PSF: $\{\mathbf{H}(s, t)\}_{s, t = -M}^M$, including the support size parameter: M . Hence, BID could be converted to BSS provided that a multichannel version of the blurred image (3) is available.

Instead of vectorizing multichannel image components of the multichannel tensor $\underline{\mathbf{G}}$ and performing BSS by matrix factorization based methods [6,7], tensor $\underline{\mathbf{G}}$ is factorized directly by using higher-order-orthogonal iteration (HOOI) algorithm [13]. For this purpose tensor $\underline{\mathbf{G}}$ is represented by Tucker3 model [14] as an n -mode product between the core tensor $\underline{\mathbf{R}} \in R^{J_1 \times J_2 \times \dots \times J_N}$ and array factors $\{\mathbf{A}^{(n)} \in R^{I_n \times J_n}\}_{n=1}^3$:

$$\underline{\mathbf{G}} \approx \underline{\mathbf{R}} \times_1 \mathbf{A}^{(1)} \times_2 \mathbf{A}^{(2)} \times_3 \mathbf{A}^{(3)} \quad (4)$$

Throughout this paper it is assumed that $J_1 = J_2 = J_3 = J$, where $J \leq \min\{I_1, I_2, I_3\}$. Since the core tensor $\underline{\mathbf{R}}$ allows interaction of a factor with any factor in the other modes, the Tucker3 model is flexible in modeling complex interactions within the data tensor $\underline{\mathbf{G}}$. This, however, prevents the uniqueness of its decomposition (4). However, imposing orthogonality constraints on array factors and all-orthogonality and ordering constraints on the core tensor in (4), as it is done by the HOOI algorithm, yields factorization that is virtually unique. Dimensionality analysis of the multichannel image tensor $\underline{\mathbf{G}}$ implies that $\mathbf{A}^{(3)}$ corresponds with the mixing matrix while

$$\hat{\underline{\mathbf{F}}} \approx \underline{\mathbf{R}} \times_1 \mathbf{A}^{(1)} \times_2 \mathbf{A}^{(2)} = \underline{\mathbf{G}} \times_3 (\mathbf{A}^{(3)})^\dagger \quad (5)$$

yields an estimate of the tensor $\underline{\mathbf{F}} \in R^{I_1 \times I_2 \times J}$ comprising the original image and its spatial derivatives. Hence, by using HOOI algorithm blind separation of the original image and its spatial derivatives is achieved without imposing on them hard constraints such as mutual sparseness (disjoint support) or statistical independence.

III. SINGLE-FRAME IMAGE DECONVOLUTION USING CONTINUOUS WAVELET TRANSFORM

In general, it is difficult to conduct image restoration or sharpening based on a single-frame image due to the lack of additional information for the scene. It is easier if more observations are available about the scene, and image details can be extracted from these observations. Here, we investigate a single-frame multi-channel image enhancement approach. Gabor filter bank with two spatial frequencies and four orientations has been used for this purpose in [6-10]. In this paper, we propose the use of the CWT at the proper scale a and shift b :

$$\mathbf{G}_{i_3(a,b)}(i_1, i_2) = \frac{1}{\sqrt{a}} \int_{-\infty}^{\infty} \mathbf{G}(t(i_1, i_2)) \psi\left(\frac{t(i_1, i_2) - b}{a}\right) dt \quad (6)$$

It is clear from notation in (6) that degraded image \mathbf{G} is vectorized before 1D CWT is applied to it and $t(i_1, i_2)$ represents new index in 1D representation. It follows from (6) that selecting scale a and shift b new set of degraded images is obtained:

$$\mathbf{G}_{i_3}(i_1, i_2) = a_{i_3 1}\mathbf{F}(i_1, i_2) - a_{i_3 2}\mathbf{F}_{i_1}(i_1, i_2) - a_{i_3 3}\mathbf{F}_{i_2}(i_1, i_2) + a_{i_3 4}\mathbf{F}_{i_1 i_1}(i_1, i_2) + a_{i_3 5}\mathbf{F}_{i_2 i_2}(i_1, i_2) + a_{i_3 6}\mathbf{F}_{i_1 i_2}(i_1, i_2) - \dots \quad (7)$$

where expressions for weighting coefficients are straightforward to derive and can also be found in [6,7]. In (7) explicit dependence of the multichannel image index i_3 on scale a and shift b is dropped to simplify notation. In the experiments reported in section 4 the shift parameter b was set to zero.

Hence, after CWT, a multichannel image tensor $\underline{\mathbf{G}} \in R_{0+}^{I_1 \times I_2 \times I_3}$ is obtained, which comprises blurred image \mathbf{G} and $(I_3 - 1)$ images generated by the CWT transform. The HOOI algorithm in section 3 is applied to $\underline{\mathbf{G}}$, and the decomposed image with the best quality is the final output. The proposed method is called CWT-HOOI algorithm.

IV. EXPERIMENTAL RESULTS

An image of the Washington Monument in Fig. 1(a) was used in the first experiment. Fig. 2 shows the sixteen 1D CWT-generated images using the Mexican hat wavelet with different directions and scaling factors. Basically, the multichannel version highlighted the details in the original image. However, with the increasing of the scaling factor a , the image was somewhat blurred, and a small scaling factor

may highlight noise. So, in general, $[0.5, 2]$ is an appropriate range for the value of a . The type of wavelets also played a role. Fig. 3 shows the Morlet wavelet generated images (along the horizontal direction). Compared to Fig. 2(a), the Morlet wavelet may yield more artifacts than the Mexican hat. Hence, we will use the Mexican hat wavelet hereafter. Fig. 1(b) and (c) show the restoration result using the blind Richardson-Lucy (RL) method with the assumption that the PSF support size was three or five, and PSF had a Gaussian kernel. Compared to the original image in Fig. 1(a), there was no much difference. Fig. 1(d) is the result from CWT-HOOI using the image tensor consisting of the original and the sixteen images in Fig. 2. We can see the image was slightly improved with texture information in the monument becoming more visible.

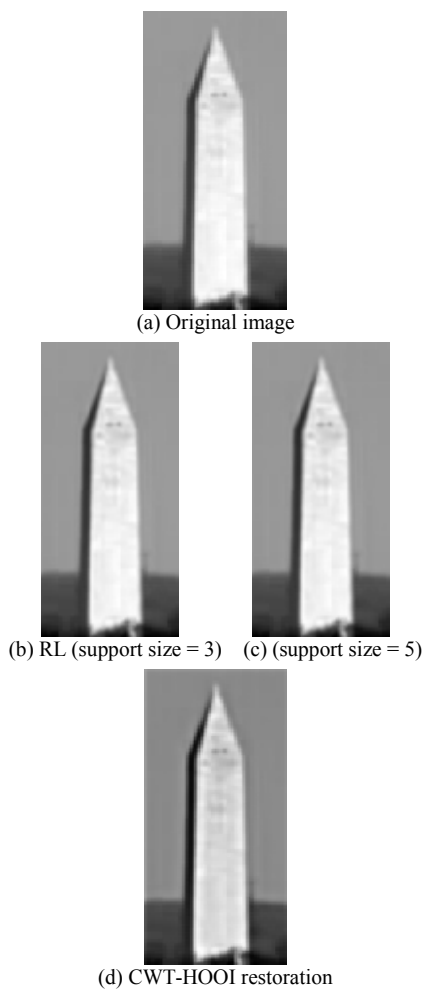


Figure 1. The original and restored images in the first experiment.

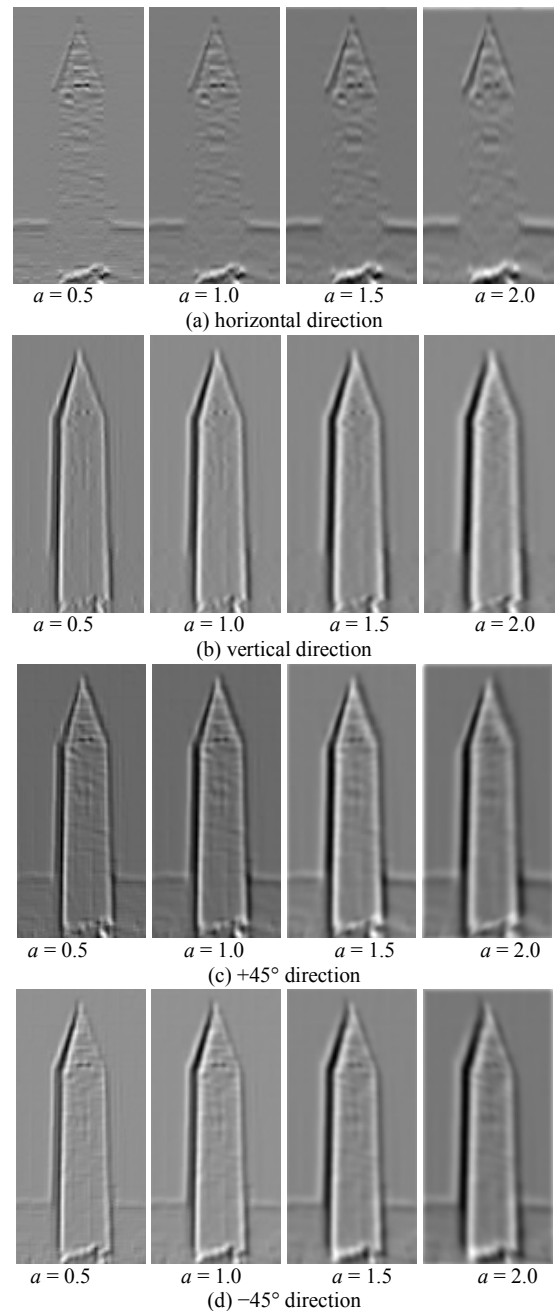


Fig. 2. CWT-generated multichannel version of Fig. 1(a) (with the Mexican hat wavelet).

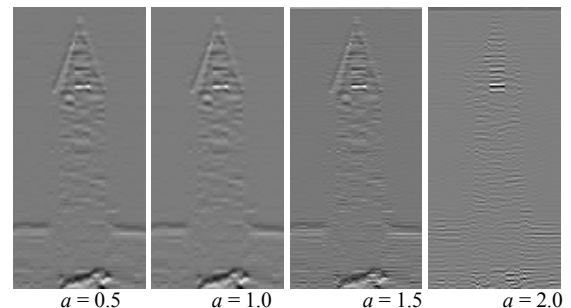
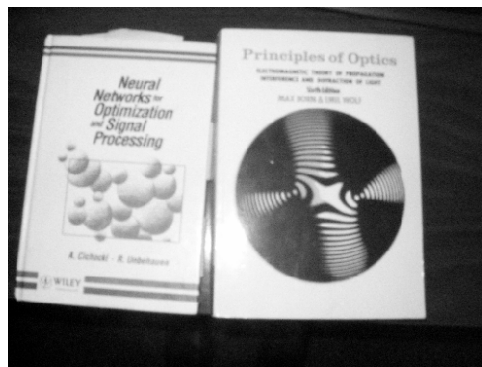
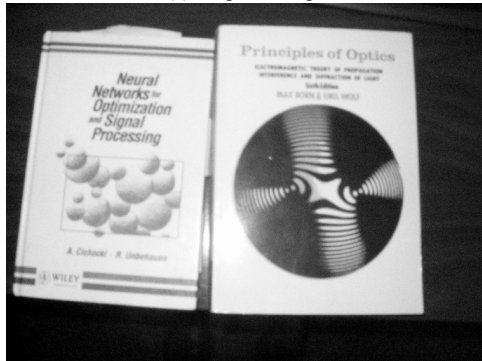


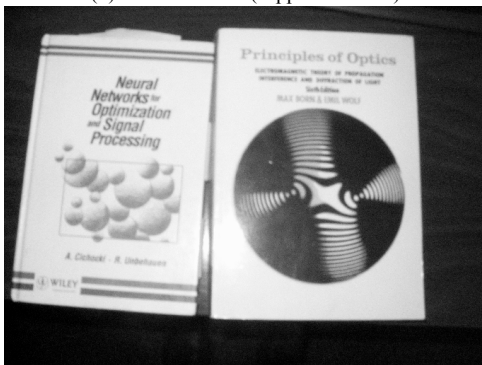
Fig. 3. CWT-generated multichannel version (along horizontal direction) of Fig. 1(a) (with the Morlet wavelet).



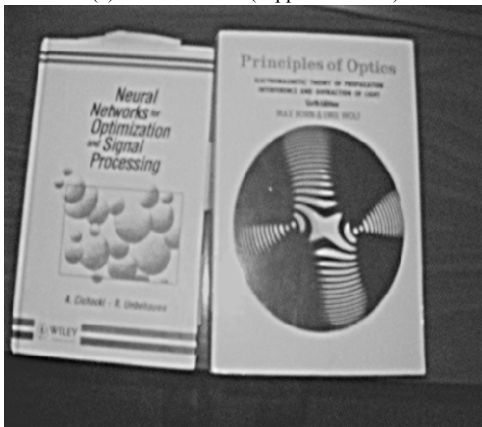
(a) Original image



(b) RL restoration (support size = 3)



(c) RL restoration (support size = 5)



(d) CWT-HOOI restoration

Fig. 4. The original and restored images in the second experiment.

In the second experiment, the original image was blurred due to defocusing as shown in Fig. 4(a). The blind RL restoration result in Fig. 4(b) and (c) did not show any improvement. The proposed CWT-HOOI result shown in Fig. 4(d) presented some improvement. For instance, the desk in the background became much clearer. Here, the 1D CWT was applied to the four directions as in Fig. 2, and the value of scaling factor a was in $[0.25, 2.5]$.

V. CONCLUSION

In this paper, a blind model-free single-frame image restoration method is proposed, which virtually requires no information about the blurring kernel: neither model nor size of the support. The method uses 1D CWT to generate a multichannel version of degraded image and is followed by orthogonality constrained tensor factorization based blind source separation (the HOOI algorithm) to achieve image deconvolution for restoration. Better performance is demonstrated relative to the traditional blind RL method that, however, requires *a priori* information about the parametric model of the PSF. It is conjectured that the proposed method can be useful for the scenarios where no *a priori* information about the blurring process is available and the degradation is modest.

ACKNOWLEDGMENT

The first author is supported by grant 098-0982903-2558 funded by the Ministry of Science, Education and Sports, Republic of Croatia.

REFERENCES

- [1] R. L. Lagendijk, and J. Biemond, *Iterative Identification and Restoration of Images*, KAP, 1991.
- [2] P. Campisi, and K. Egiazarian, editors, *Blind Image Deconvolution*, CRC Press, Boca Raton, 2007.
- [3] D. Kundur, and D. Hatzinakos, "Blind Image Deconvolution," *IEEE Signal Process. Mag.*, 1996, vol. 13, pp. 43-64.
- [4] F. Li, X. Jia, and D. Fraser, "Superresolution Reconstruction of Multispectral Data for Improved Image Classification," *IEEE Geos. Rem. Sens. Lett.*, 2009, pp. 689-693.
- [5] D. A. Fish, A. M. Brinicombe, E. R. Pike, and J. G. Walker, "Blind deconvolution by means of the Richardson-Lucy algorithm," *J. Opt. Soc. Am. A*, 1995, vol. 12, pp. 58-65.
- [6] I. Kopriva, "Single Frame Multichannel Blind Deconvolution by Non-negative Matrix Factorization with Sparseness Constraint," *Opt. Lett.*, 1995, vol. 30, pp. 3135-3137.
- [7] I. Kopriva, "Approach to Blind Image Deconvolution by Multiscale Subband Decomposition and Independent Component Analysis," *J. Opt. Soc. Am. A*, 2007, vol. 24, pp. 973-983.
- [8] Q. Du, and I. Kopriva, "Dependent component analysis for blind restoration of images degraded by turbulent atmosphere," *Neurocomputing*, 2009, vol. 72, pp. 2682-2692.
- [9] I. Kopriva, "3D tensor factorization approach to single-frame model-free blind-image deconvolution," *Opt. Lett.*, 2009, vol. 34, pp. 2835-2837.
- [10] I. Kopriva, "Tensor Factorization for model-free space-variant blind deconvolution of the single- and multi-frame multi-spectral Image," *Optics Express*, 2010, vol. 18, No. 17, pp. 17819-17833.

- [11] S. Umeyama, "Blind Deconvolution of Blurred Images by Use of ICA," *Electron Comm Jpn*, 2001, vol. 84, No. 12, pp. 1-9.
- [12] P. S. Addison, *The Illustrated Wavelet Transform Handbook*, Taylor & Franics, 2002.
- [13] L. De Lathauwer, B. De Moor, and J. Vandewalle, "On the best rank-1 and rank-(R_1, R_2, \dots, R_N) approximation of higher-order tensors," *SIAM J. Matrix Anal. and Appl.*, 2000, vol. 21, pp. 1324-1342.
- [14] L. R. Tucker, "Some mathematical notes on three-mode factor analysis," *Psychometrika*, 1966, vol. 31, pp. 279-311.